XANES speciation of P in environmental samples: an assessment of filter media for on-site wastewater treatment.

David Eveborn,†, Jon Petter Gustafsson†, Dean Hesterberg‡, Stephen Hillier*

†Department of Land and Water Resources Engineering, Royal Institute of Technology, SE-100 44 Stockholm, Sweden

‡Department of Soil Science, Box 7619, North Carolina State University, Raleigh, North Carolina 27695-7619

Macaulay Institute, Craigiebuckler, Aberdeen AB15 8QH, Aberdeen, U.K.

*Corresponding author's phone: +46 8 790 73 28, e-mail: eveborn@kth.se

Abstract

X-ray absorption near edge structure (XANES) is a useful technique for characterisation of chemical species of phosphorus in complex environmental samples. To develop and evaluate

bed filters as sustainable on-site wastewater treatment solutions, our objective in this study was to determine the chemical forms of accumulated phosphorus in a selection of promising filter materials: Filtralite P, Filtra P, Polonite, Absol, blast furnace slag, and wollastonite. Full-scale operational wastewater-treatment systems were sampled and in addition, filter samples collected from laboratory studies provided access to additional media and complementary samples. Phosphorus species were characterized using phosphorus K-edge XANES spectroscopy, complemented by X-ray powder diffraction (XRPD) and attenuated total reflectance Fourier-transform infrared spectroscopy (ATR-FTIR). No systematic differences could be seen in the results between laboratory- and full-scale samples. All six filter media contained significant amounts of crystalline calcium phosphates. Some samples also contained amorphous calcium phosphate (>60% of total P in Absol). In Filtralite P and blast furnace slag, more than 35% of the accumulated phosphorus was associated with Fe or Al. Both the power and shortcomings of XANES analysis for characterizing P species in these filter media are discussed.

Introduction

Phosphorus availability is critical to the issue of eutrophication in many inland waters and even some coastal seas (1). To reduce the phosphorus loads to natural waters, various filter media have been explored for their capacity to remove P from wastewater (2) (primarily from on-site systems), urban runoff, landfill leachate and agricultural runoff. Phosphorus accumulated in exhausted filters may be recycled to agriculture, ultimately a more efficient use (3).

The majority of the filter media that are effective P sorbents are alkaline and contain calcium-rich minerals. Chemical mechanisms of P removal mechanisms by these media have been studied to some extent (4-7), but remain poorly understood. Knowledge of the chemical

speciation and reactivity is critical for optimizing and predicting the behavior of bed filter systems, both during utilization as well as during any subsequent recycling phase. These aspects are also important when trying to evaluate the performance of the bed filter technique with respect to other on-site treatment technologies by means of life cycle assessment methodologies (8).

This study aims to identify the chemical forms (species) of accumulated P in filter media used for on-site treatment of wastewater. Knowledge about P species in exhausted filter media will not only provide information about removal mechanisms, but also provide insights into the performance of these media as a fertilizer when recycled to agriculture. Both aspects are relevant for the development and evaluation of bed filters as sustainable on-site wastewater treatment solutions.

Phosphorus K-edge X-ray absorption near edge structure (XANES) spectroscopy, complemented by X-ray powder diffraction (XRPD) and attenuated total reflectance Fourier-transform infrared spectroscopy (ATR-FTIR) were used as analytical tools in this study. Only a few researchers have tried to identify the trapped P compounds in filter applications, and only for a limited number of filter media. Analysis methods used previously include ATR-FTIR (4), XRPD (6; 9), chemical fractionation, and scanning electron microscopy (SEM) with energy-dispersive X-ray spectroscopy (EDS) (6).

X-ray absorption spectroscopy (XAS) is useful for characterizing chemical species of P in complex environmental samples (10). Spectra are derived from changes in the X-ray absorption coefficient around the X-ray absorption edge of an element of interest (the absorber). Edge energies are unique for different chemical elements, so XAS is element specific. Spectral features near the edge depend on the average local coordination environments of all absorber atoms in the sample (10). XAS can be utilized with minimal sample preparation, which makes it suitable for phosphorus speciation in environmental

samples. Phosphorus K-edge XANES studies have provided insights into the P speciation in, e.g., dairy manure (11), poultry litter (12-13) and soils (14-16).

Experimental section

Six different filter media were evaluated in this study. Brief descriptions and elemental compositions of these materials are presented in Table 1. All materials have previously been studied with regard to their suitability as sorbents in phosphorus removal applications.

The study was carried out with P-loaded filter samples with different loading histories (Table 2). With exception for column samples, real wastewater was used for the loading procedure. The Filtralite P column sample came from an unpublished study carried out at the Maxit Group AS in Norway and the other column samples from published research (4). The Absol (AOL) sample was derived from a small-scale box experiment carried out at the Royal Institute of Technology, Sweden (Renman et al., manuscript in preparation). Remaining samples came from full scale operational systems.

Synthetic wastewater does not contain many potentially important components such as complex mixtures of organic substances and salts that are typically found in actual wastewaters. However, no field-deployed samples of the water-cooled blast furnace slag (BFS) and wollastonite (WTE) were available, so these samples were treated only with synthetic wastewater in columns. On other hand, it has been reported that the role of organic substances for the precipitation of calcium phosphates is very limited at pH > 9 (18). Wastewaters used during the P-loading of the samples are described in SI Table S1.

Attenuated Total Reflectance Fourier-Transform Infrared Spectroscopy. To verify purity, standards used in the XANES analysis were also analyzed by ATR-FTIR using a

Perkin-Elmer S2000 FTIR spectrometer equipped with a Golden-Gate diamond cell. Before analysis, the samples were air- or freeze-dried and gently crushed in a mortar.

X-ray powder diffraction. X-ray powder diffraction data were collected on an analytical X-pert Pro laboratory diffractomer. Ni filtered Cu Kα radiation was used with the incident beam collimated with soller slits, ¼-degree divergence slit, 10 mm beam mask, and a ¼-degree antiscatter slit. The diffracted beam was collimated with a beam tunnel and diffracted beam soller slits. The powder samples were mounted in 16 mm circular holders, and an antiscatter beam knife was mounted above the sample. The samples were rotated at 60 rpm while being scanned from 5 to 70° 2Θ, with counting times of 100 s per 0.167 degree step taken using an X-celerator position sensitive detector. If necessary, the samples were gently ground by hand in an agate mortar and pestle to ensure that they were of a suitably fine grain size for XRPD.

Preparation of XANES standards. For the interpretation of XANES data, standard spectra for the following eight different inorganic phosphate compounds were used: amorphous calcium phosphate (ACP), octacalcium phosphate (OCP), hydroxyapatite (HA), brushite (BTE), monetite (MTE), hydrated aluminium phosphate (AlP), phosphate adsorbed to aluminum oxide (boehmite) (Alox-P) or ferrihydrite (Feox-P).

Octacalcium phosphate was synthesized at 42 ^{o}C using the method of Christoffersen et al. (19). These authors also presented methods to synthesize two versions of ACP termed ACP1 and ACP2. However, the use of these methods at our laboratory produced significant amounts of poorly crystalline OCP in the samples based on ATR-FTIR and XRPD analyses.

Instead, ACP was synthesized at 30 ^{o}C by adding 12.5 mmol $Ca(OH)_2$ to 5 dm^3 of 0.5 mM K_2HPO_4 giving a Ca:P ratio of 5:1. The solution pH increased to 10.57 during the addition of

$Ca(OH)_2$. The mixture was agitated for 8 min. After sedimentation of the precipitated particles, the clear, supernatant liquid phase was removed. The remaining suspension was filtered, and the filter was then freeze-dried to prevent crystallization. The sample was put in the freeze-drier 1.5 h after the reaction was initiated.

Synthesis of hydrated aluminum phosphate $AlPO_4 \bullet 1.5\ H_2O$ was done according to Lagno and Demopolus (20). Spectra for the five remaining standards were collected on mineral or adsorbed P standards prepared as described in earlier P K-edge XANES studies (14; 21). The purity of the two synthesized calcium phosphates was verified by XRPD and ATR-FTIR analysis.

Sample preparation for XANES analysis. Column samples had been stored at $+4^oC$ for about 1 year and wastewater-treated samples were stored for < 1 month before they were prepared for XANES data collection.

The samples were dried (freeze-dried or air-dried) before further preparation. To concentrate P in field samples containing low amounts of accumulated P, the media were shaken over a screen to disaggregate and collect exterior particles of the grains/granules. The samples were finally sieved using a 42 µm sieve. To reduce self-absorption effects due to the low X-ray energies at the P K-edge, all samples containing >800 mmol P kg^{-1} were diluted in petroleum jelly to achieve a concentration of ≤400 mmol P kg^{-1}. To ensure uniform mixing, subsamples were added into a given amount of petroleum jelly in a porcelain vessel, and the sample was mixed very thoroughly to eliminate clumps and disperse the sample.

XANES data collection and data treatment. The XANES data were collected at Beamline X-15B at the National Synchrotron Light Source, Brookhaven National Laboratory, Upton, NY. The beamline was operated in fluorescence mode and the fluorescence signal was

measured using a solid state Ge fluorescence detector. The sample and X-ray flight path inside the sample compartment was purged with He gas.

Correction of any shifts on energy scale caused by monochromator drift was made by periodically collecting standards of variscite or ACP during each beamtime. All samples and standards were calibrated to a common energy scale by setting the maximum of the first derivative spectrum of variscite to 2151 eV (10). Any differences in the first-derivative maxima in the samples and standards (defined as E_0 for data normalization) should therefore be spectral shifts attributable to local molecular bonding.

The scans ranged from 2100 eV to 2600 eV with a smaller energy-step size and longer counting time over areas of interest (0.1 eV step and 5 s counting time over the absorption edge). Depending on the level of noise in spectra, three to six scans per sample were collected and merged.

Merged spectra were normalized using a consistent procedure across all sample spectra, the details of which can be found elsewhere (10). In brief, a linear baseline function was subtracted from the spectral region below the edge (typically between 2100 and 2135 eV), and spectra were normalized to unit edge step and quadrature removed across the post-white-line region (typically between 2200 and 2450 eV) to obtain a normalized XANES spectrum.

XANES Fitting Analysis. A linear combination fitting (LCF) approach (22) was used to determine combinations of standard spectra giving the best fit to the sample spectra. All data were analyzed using the Athena software (v0.8.056) (23). No energy shifts were permitted in the LCF fitting algorithm and the weighting factors were not forced to sum to one.

The fitting was performed in a number of steps. Fitting the data in first derivative space with a wide fitting range of -5 to 30 eV relative to the white line derived a qualitative overview. In the next step, sample spectra with fits indicating >2% Fe-associated P were again fitted but in normalized XANES space, to the same standards used in the derivative fits.

In this case, the energy range of the fitting was constrained at -5 to -1 eV, a unique region for determining iron associated P. If a fit in this region revealed <1% of total P associated with Fe, then the Fe standard was abandoned for the particular sample. In addition components identified by XRPD in a sample were treated as required components in the XANES fitting. The fitting range was then again expanded to the wide region (-5 to 30 eV), and a final fit that implemented the new constraints was performed. To determine likely forms of Ca-associated P, isolated fits in first derivative space were performed in a region between 2 eV and 23 eV relative to the white line.

Results

XRPD and ATR-FTIR Characterization of Standards. An example of XRPD and ATR-FTIR results are shown in Figure 1 for ACP. XRPD data show two broad regions of scattering centered at approximately 30^{o} and 47° 2Θ, which is characteristic for ACP (24, 25). However, peaks indicating a minor amount of calcite were also present, apparently due to CO_2 contamination during or after synthesis. The ATR-FTIR spectrum contained single broad P-O bands at 552 cm^{-1} and at 1010 cm^{-1}, as expected for ACP (24, 25), and a minor amount of . calcite was also indicated by a carbonate band at 874 cm^{-1} (Figure 1).

Phosphorus phases as evidenced by XRPD. In most XRPD patterns of filter samples, P species were undetectable, probably because the concentration of any P minerals was too low to detect. One exception was the PTE1 sample, where the presence of a poorly crystallized HA could be confirmed (Figure 2). The XRPD peak at approximately 10.8° 2Θ is absent, and a doublet at approximately 9.3 and 9.7° 2Θ is present along with other distinguishing peaks.

XANES spectra for standards. The calcium phosphates are characterized by a post-white line shoulder at around 2153.5 eV (Figure 3). The shoulder is more pronounced for the more crystalline standards such as HA and OCP than for ACP. The crystalline phases can also be distinguished from ACP by the presence of a minor post-white line peak at 2162 eV. In brushite, a single peak occurs at ~0.8 eV above the post-white line shoulder. Moreover brushite shows an additional post-white line peak at 2161.5 eV. The shoulder for monetite is embedded in the white line causing asymmetry on the high-energy side of the white line.

The spectrum representing iron-associated phosphates has a significant pre-white line peak at around 2146 eV, while the aluminum-associated phosphate lacks discernible pre- and post-white line features. Our observations are in line with other studies (11; 14; 26, 27).

Phosphorus Phases in Filter Samples as Shown by XANES. A representative subset of three of the ten sample spectra and final fits are shown in Figure 4 (the remaining seven spectra plus fits are shown in SI Figure S1). Using the unique pre-white line feature for Fe(III)-bonded PO_4 -5 eV to -1 eV (relative energy), Fe(III)-associated P was confirmed only for the FTE2, FAP2 and WTE samples. Hence, Fe-bound P standards were required for these samples and eliminated for others. In addition to this constraint, HA was required in the PTE1 sample based on XRPD results. Results summarized in Table 3 are based on wide-range fits between -5 eV and 30 eV (relative energy) in first derivative space, implementing the described constraints. For these results, the sums of weighting factors on standards derived from the fitting result were subsequently normalized to 1 (14).

For all investigated samples, the XANES fitting results indicated significant amounts of crystalline calcium phosphates (OCP or HA). The Filtra P and AOL samples also contained a substantial amount (>25%) of ACP (for AOL as much as 63%) and the Filtralite P, BFS, and WTE samples >35% (in total) of Fe- and/or Al-associated P. No systematic differences

between P phases in samples loaded with real wastewater versus synthetic wastewater could not be found.

In most cases, the dominating P components indicated by XANES fitting were consistent across many of the five best fits (Table 3). However, spectral differences between OCP and HA are subtle. A comparison between the poorly crystalline OCP as used in this investigation with a more crystalline OCP sample revealed larger differences in the XANES spectra than between crystalline OCP and crystalline HA (spectra not shown). This similarity can explain why OCP and HA often appeared together or as substitutes for each other in the bests fits for a given sample. There seems to be no reliable way of distinguishing between HA and OCP using the P K-edge XANES technique (certainly within the current study).

To qualify the XANES fitting results with respect to Ca-phosphate components, a constrained fit was performed over a range between 2 eV and 23 eV relative to the edge. Except for some disagreement in the modeled partitioning of HA relative to OCP, no significant qualitative differences were observed for the FTE2, FAP1, FAP2, and AOL samples. However differences to the wide range fit could be seen for FTE1 and PTE2, for which large proportions of ACP were identified in the constrained fit (SI Table S2). Furthermore, the constrained fit in contrast to the wide range fit indicated significant amounts of monetite in the FAP3, BFS and WTE samples.

The Ca-phosphate standards used in out XANES fitting are not easily distinguished from each other due to lack of unique features. As an example, the post-white-line shoulder region can be fit with either ACP or a combination of boehmite-associated P and OCP or HA. This lack of uniqueness resulted in difficulty to discriminate between Ca phosphates when fitting some samples across the limited region (2 - 23 eV relative energy). However, since the smaller step sizes yield more data points across the edge region, fitting across a wide spectral

region (e.g., -5 to 30 eV relative energy) results in less sensitivity and perhaps suboptimal fits to subtler features in the post-white-line region.

Discussion

Phosphorus Speciation in Filter Media. Consistent with other investigations (4), this study confirms that Ca-phosphate precipitation is important for removal of P from wastewater by alkaline filter materials. In some cases (particularly for the BFS and Filtralite P materials) a substantial part of the bound phosphorus was also associated with Al and Fe phases. However, the results presented here do not provide the whole picture since they do not distinguish the pathway by which the final P phases were formed. At higher pH ranges it has been reported that initial precipitates of ACP over time will transform to HA (28, 29). However, the crystallization process may be inhibited or delayed by the presence of complexing organic substances in the wastewater (18;30, 31). The pH value would be expected to be important for the phase composition of P. In Filtra P, Polonite, and Filtralite P, the pH is usually very high initially and gradually decreases during operation (*e.g.*, refs 4, 17). In such an environment, Ca phosphates would be expected to form. In BFS and wollastonite, the operational pH is lower (<9, note that the operational pH for the WTE sample was ~8, i.e. lower than the pH at equilibrium given in Table 2), which is consistent with a more pronounced tendency for P to be adsorbed and/or precipitated with Al and Fe phases. It is possible, however, that major changes in P speciation may occur when alkaline filter media such as Filtra P, Polonite and Filtralite P are exhausted, at which point the pH value could fall below pH 9. A pH decline would tend to cause dissolution of Ca phosphates, particularly ACP (4). This effect may explain the minor amount of Al- and Fe-bound P in the FAP1, FAP3 and PTE2 samples, and of a major contribution of these phases in the FTE2 sample. However, Al- and Fe associated P was also present in significant quantities in FTE1, despite

the pH being greater than 9 when it was sampled. Hence, the contribution of Al and Fe (hydr)oxides to P binding seem to be important for Filtralite even at higher pH.

From a P recycling perspective it would be preferable to capture phosphorus from wastewater in an easily soluble fraction readily available to plants. ACP would then be preferable to the more crystalline calcium phosphates HA or OCP. The Al- and Fe-associated P species are likely to be less soluble than the Ca phosphates, especially in acidic soils. However, plant availability is a complex issue that cannot be assessed from the phosphorus species in the recycled material only. In essence, plant availability of P from filter materials will depend on properties of the agricultural soil, any material preprocessing (such as grinding or mixing with other soil amendments), and chemical and biological processes that regulate plant uptake.

Interpretation of XANES Spectra. For low-energy edges such as the phosphorus K-edge, differences in X-ray absorption by the purge gas in the flight path at different energies can potentially cause spectral distortions, so a consistent normalization procedure should be used for all samples and standards. Complementary measurements like XRPD and ATR-FTIR can constrain the selection of standards to better represent standards in the sample. Spectral distortions due to self-absorption (22) are also an issue, particularly at low energies. Concentrated samples such as standards should be diluted and dispersed in micrometer-sized particles, or mounted as thin (10s of micrometers) samples that transmit a significant proportion of the incident X-rays.

The LCF approach presupposes that it is valid to break up the sample data into parts of the pure components used in fitting. This supposition has been explicitly verified for some phosphorus compounds by empirical experiments (32). However, when working with environmental samples, it is still an assumption that standards are representative for the actual P-species in the sample.

The LCF optimization method of the Athena software uses a numerical function that minimizes the sum of the deviations between data and model fit over all individual data points across the energy region being fit in the XANES spectrum. This approach, when performed on normalized data, is not feature sensitive (the absolute fluorescence intensity dictates the fit more than the curvature of spectral features). Therefore, the result will be a forced intensity overlay without any specific attempts to respect the curvature. Particularly if data are distorted due to problems with normalization or inconsistencies in self-absorption, it should be preferable to use a fitting algorithm that prioritizes curvature over absolute intensity to better distinguish species based on unique spectral shapes (features). Fitting first-derivative spectra as presented in this study satisfies this criterion. For the PTE1 sample for example, derivative fitting resulted in an excellent representation of the spectral shape, even though the fluorescence intensity was not equally well described (Figure 4c). Fits to some samples (Supporting Information) showed an even greater discrepancy between normalized and derivative XANES fits. We believe that fitting in first-derivative space is a more forgiving and sensitive method for discriminating possible species, particularly when spectral distortions are a concern. A significant discrepancy between intensities of fits and normalized XANES data might be interpreted as either data distortion or nonrepresentative standards. Although quantitative uncertainty of such results can be high, qualitative aspects should be sound.

When fitting either normalized or derivate XANES spectra, the relative weights given to different parts of the spectrum should be recognized. As stressed in the built-in manual for the Athena software, regions of spectra sampled with smaller step sizes (generally the white line region) will receive greater weighting in the fitting process than other regions. As shown here, performing a sequence of fits across different, characteristic regions of XANES spectra can be helpful for validation.

Acknowledgements

We credit Paul Northrup, beamline scientist at X15b, NSLS, for his support during XANES data collection. Kimberly Hutchison, NCSU, is acknowledged for practical assistance and providing us with variscite and Gunno Renman, KTH, for giving us various filter materials from laboratory and field experiments and criticism on the manuscript. Also many thanks are due to Nordkalk Oyj Abp and Maxit Group AS who helped us find suitable filter media of their products. The Swedish Research Council Formas (Project No. 2006-632), are acknowledged for financial support of this research. S.H. acknowledges the support of the SEERAD. Finally, this research was carried out (in part) at the National Synchrotron Light Source (NSLS), Brookhaven National Laboratory, which is supported by the U.S. Department of Energy, Division of Materials Sciences and Division of Chemical Sciences.

Supporting Information Available

LCF results for samples not shown in the article and tables comparing wastewaters for P-loading and results from wide range and constrained range fitting. This material is available free of charge via the Internet at http://pubs.acs.org.

Literature Cited

(1) Smith, V. H. Eutrophication of freshwater and coastal marine ecosystems - a global problem. *Environ. Sci. Pollut. Res.* **2003**, 10, 126–139.

(2) Johansson Westholm, L. Substrates for phosphorus removal - Potential benefits for on-site wastewater treatment? *Water Res.* **2005**, 40, 23–36.

(3) Cucarella, V.; Zaleski, T.; Mazurek, R.; Renman, G. Effect of reactive substrates used for the removal of phosphorus from wastewater on the fertility of acid soils. *Bioresour. Technol.* **2008**, 99, 4308-4314.

(4) Gustafsson, J. P.; Renman, A.; Renman, G.; Poll, K. Phosphate removal by mineral-based sorbents used in filters for small-scale wastewater treatment. *Water Res.* **2008**, 42, 189–197.

(5) Pratt, C.; Shilton, A., Pratt, S.; Haverkamp, R. G.; Elmetri, I. Effects of redox potential and pH changes on phosphorus retention by melter slag filters treating wastewater. *Environ. Sci. Technol.* **2007**, 41, 6585–6590.

(6) Pratt, C.; Shilton, A.; Pratt, S.; Haverkamp, R. G.; Bolan, N. Phosphorus removal mechanisms in active slag filters treating waste stabilization pond effluent. *Environ. Sci. Technol.* **2007**, 41, 3296-3301.

(7) Johansson, L.; Gustafsson, J. P. Phosphate removal using blast furnace slags and opoka-mechanisms. *Water Res.* **2000**, 34, 259–265.

(8) Weiss, P.; Eveborn, D.; Kärrman, E.; Gustafsson J.P. Environmental systems analysis of four on-site wastewater treatment options. *Resour. Conserv. Recycl.* **2008**, 52, 1153–1161.

(9) Lu, S. G.; Bai, S. Q.; Shan, H. D. Mechanisms of phosphate removal from aqueous solution by blast furnace slag and steel furnace slag. *J. Zhejiang Univ. Sci. A* **2008**, 9, 125–132.

(10) Kelly, S.; Hesterberg, D.; Ravel, B. Analysis of soils and minerals using x-ray absorption spectroscopy. In *Methods of Soil Analysis*; Ulery, A.L., Drees, R., Eds.; Soil Science Society of America: Madison, WI, 2008; pp. 387–463.

(11) Güngör, K.; Jürgensen, A.; Karthikeyan, K. G. Determination of phosphorus speciation in dairy manure using XRD and XANES spectroscopy. *J. Environ. Qual.* **2007**, 36, 1856–1863.

(12) Peak, D.; Sims, J. T.; Sparks, D. L. Solid-state speciation of natural and alum-amended poultry litter using XANES spectroscopy. *Environ. Sci. Technol.* **2002**, 36, 4253–4261.

(13) Seiter, J. M.; Staats-Borda, K. E.; Ginder-Vogel, M.; Sparks, D. L. XANES spectroscopic analysis of phosphorus speciation in alum-amended poultry litter. *J. Environ. Qual.* **2008**, 37, 477–485.

(14) Beauchemin, S.; Hesterberg, D.; Chou, J.; Beauchemin, M.; Simard, R. R.; Sayers, D. E. Speciation of phosphorus in phosphorus-enriched agricultural soils using x-ray absorption near-edge structure spectroscopy and chemical fractionation. *J. Environ. Qual.* **2003**, 32, 1809–1819.

(15) Sato, S.; Solomon, D.; Hyland, C.; Ketterings, Q. M.; Lehmann, J. Phosphorus speciation in manure and manure-amended soils using XANES spectroscopy. *Environ. Sci. Technol.* **2005**, 39, 7485–7491.

(16) Ajiboye, B.; Akinremi , O. O. ; Hu, Y.; Jürgensen, A. XANES speciation of phosphorus in organically amended and fertilized vertisol and mollisol. *Soil Sci. Soc. Am. J.* **2008**, 72, 1256–1262.

(17) Adam, K.; Krogstad, T., Vrale; L., Sovik, A. K.; Jenssen, P. D. Phosphorus retention in the filter materials shellsand and Filtralite P® - batch and column experiment with synthetic p solution and secondary wastewater. *Ecol. Eng.* **2007**, 29, 200–208.

(18) Song, Y. H.; Hahn, H. H.; Hoffmann, E.; Weidler, P. G. Effect of humic substances on the precipitation of calcium phosphate. *J. Environ. Sci.* **2006**, 18, 852–857.

(19) Christoffersen, M. R.; Christoffersen, J.; Kibalczyc, W. Apparent solubilities of two amorphous calcium phosphates and of octacalcium phosphate in the temperature range 30-42ºC. *J. Crystal Growth* **1990**, 106, 349–354.

(20) Lagno, F.; Demopoulos, G. P. The stability of hydrated aluminium phosphate, $AlPO_4 \cdot 1.5\ H_2O$. *Environ. Technol.* **2006**, 27, 1217–1224.

(21) Khare, N.; Hesterberg, D.; Beauchemin, S.; Wang, S. L. XANES determination of adsorbed phosphate distribution between ferrihydrite and boehmite in mixtures. *Soil Sci. Soc. Am. J.* **2004,** 68, 460-469.

(22) Tannazi, F.; Bunker, G. Determination of chemical speciation by XAFS. *Physica Scripta* **2005**, 115, 953–956.

(23) Ravel, B.; Newville, M. ATHENA, ARTEMIS, HEPHAESTUS: data analysis for X-ray absorption spectroscopy using IFEFFIT. *J. Synchrotron Rad.* **2005**, 12, 537–541.

(24) Layrolle, P.; Ito, A. Tateishi, T. Sol-gel synthesis of amorphous calcium phosphate and sintering into microporous hydroxyapatite bioceramics. *J. Am. Ceram. Soc.* **1998**, 81, 1421-1428.

(25) Li, Y. B.; Wiliana, T.; Tam, K. C. Synthesis of amorphous calcium phosphate using various types of cyclodextrins. *Mat. Res. Bull.* **2007**, 42, 820–827.

(26) Hesterberg, D.; Zhou, W. Q.; Hutchison, K. J.; Beauchemin, S.; Sayers, D. E. XAFS study of adsorbed and mineral forms of phosphate. *J. Synchrotron Rad.* **1999**, 6, 636–638.

(27) Khare, N.; Martin, J. D.; Hesterberg, D. Phosphate bonding configuration on ferrihydrite based on molecular orbital calculations and XANES fingerprinting. *Geochim. Cosmochim. Acta* **2007,** 71, 4405-4415.

(28) Kim, S.; Ryu, H. S.; Jung, F. S.; Hong, K. S. Influence of Ca/P ratios of starting solutions on the crystallization of amorphous calcium phosphate to hydroxyapatite. *Met. Mater. Int.* **2004**, 10, 171–175.

(29) Lazic, S. Microcrystalline Hydroxyapatite formation from alkaline solutions. *J. Crystal Growth* **1995**, 147, 147–154.

(30) Alvarez, R.; Evans, L. A.; Milham, P. J.; Wilson, M. A. Effects of humic material on the precipitation of calcium phosphate. *Geoderma* **2004**, 118, 245–260.

(31) van der Houwen, J. A. M.; Cressey, G.; Cressey, B. A.; Valsami-Jones, E. The effect of organic ligands on the crystallinity of calcium phosphate. *J. Crystal Growth* **2003**, 249, 572–583.

(32) Ajiboye, B.; Akinremi, O. O.; Jürgensen, A. Experimental validation of quantitative XANES analysis for phosphorus speciation. *Soil Sci. Soc. Am. J.* **2007**, 71, 1288–1291.

Tables

Table 1. Description of Filter Media Investigated in This Study.

			Major elements (g/kg)				
Name	Supplier	Description	Si	Al	Ca	Fe	Reference*
Filtra P (FAP)	Nordkalk Oyj Abp, Finland	Manufactured granules made up of heated limestone, gypsum and iron.	14.6	11.1	312	41.3	(4)
Polonite (PTE)	Bioptech AB, Sweden	Thermally treated and crushed calcium-silica bedrock	241	27	245	16.5	(4)
Water-cooled blast furnace slag (BFS)	SSAB Merox AB, Sweden	By-product from the steel industry	155	69.7	216	3.11	(4)
Wollastonite (WTE)	Aros Mineral AB, Sweden	Residues from mining of wollastonite, a calcium-silicate mineral.	276	54.6	151	21.5	(4)
Filtralite P (FTE)	Maxit Group, Norway	Expanded clay aggregates doped with limestone during the thermal expansion process.	-	20.3	30.5	5.8	(17)
Absol (AOL)	Yxhult/Svesten AB, Sweden	Mixture of sand, crushed concrete and heated limestone. Marketed as sorbent for oils, paint spills etc.	232	10.0	194	8.2	†

* Reference for detailed material description

† Renman et al., manuscript in preparation

Table 2. Description of the Applications and Experimental Setups for the Different Samples, Including pH Mmeasured as the pH in the Equilibrium Solution in the Filter Media at the End of the P-Loading Procedure) and Total P Content in the Sample

Material	Sample name	Experimental setup/application setup	pH	P content** (mmol kg^{-1})
	FTE1	Column experiment*	9.6	-
Filtralite P	FTE2	Field application†‡§	7.5	84
	FAP1	Column experiment*	7.8	626
	FAP2	Field application*‡§	12.5	28
Filtra P	FAP3	Field application†¶	7.9	-
	PTE1	Column experiment*	8.2	238
Polonite	PTE2	Field application*‡	8.46	-
Absol	AOL	Small-scale box experiment†	9.25	185
Blast furnace slag	BFS	Column experiment*	8	100
Wollastonite	WTE	Column experiment*	9.3	15

* Vertical flow direction through filter material

† Horizontal flow direction through filter material

‡ Pretreatment by septic tank

§ Pretreatment by soil infiltration module.

¶ Pretreatment by package plant including aerobic chamber and simple chemical precipitation

** Measurements on FTE2 and FAP2 were made on collected exterior particles. Measurements on other samples were done on untreated material.

Table 3. Fitting Results for the Final Fit Performed in First-Derivative space with an Energy Range between -5 eV to 30 eV[a].

		ACP	OCP	HA	Alox-P	AlP	Feox-P	MTE†	BTE‡	R-factor§
FTE1	Weight (%)		62		38					0.034
	Presence*	2,5	1	2,3,4	1,2,3,4,5			3,5	5	
FTE2	Weight (%)	23	29		28		20			0.011
	Presence*	1,2,3,4	1,3,5	2,4,5	1,2	3,4,5	1,2,3,4,5			
FAP1	Weight (%)	27	60		12					0.020
	Presence*	1,2	1,2,3,4,5	3	1		5	2,3,4		
FAP2	Weight (%)	44	56							0.043
	Presence*	1,2,3,4,5	1,2	3,4,5	4		3			
FAP3	Weight (%)	38	39				23			0.017
	Presence*	1,2,3,5	1,4	2,4	5		1,2,3,4			
PTE1	Weight (%)	14	31	26				30		0.026
	Presence*	1,3,4,5	1,2,3	2,4,5	3,5		4	1,2		
PTE2	Weight (%)		61	30	9					0.060
	Presence*	2	1,2,3,4,5	1,3,4,5	1,2	4		3	5	
AOL	Weight (%)	63	37							0.024
	Presence*	1,2,3,4,5	1	2,3,4	2,4				5	
BFS	Weight (%)		39		25	37				0.025
	Presence*		1,3	2	1,2,3,4,5		3,4	4,5		
WTE	Weight (%)		69			12	19			0.031
	Presence*	5	1,2,3,4,5	3	1,2,3,5		1,4	2,4		

a The table presents the weights of components in the best fit and the components identified in the 1st to 5th best fits.

* The presence of the particular compounds in the five best fits numbered 1 to 5. The lower the number the better fit.

† Monetite standard

‡ Brushite standard

§ The R-factor reported by the Athena software (see Athena Users' Manual for details). The lower the value the better fit (mathematically).

Figures

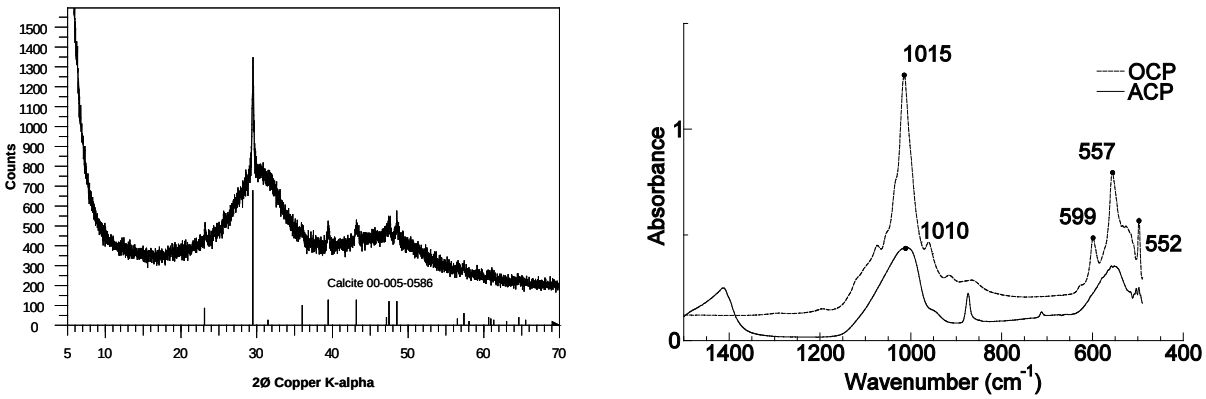

Figure 1. XRPD pattern (left) and ATR-FTIR spectrum (right, solid line) of the amorphous calcium phosphate (ACP) standard. Broad bands of scattering in the XRPD pattern are due to ACP, peaks are due to minor calcite contamination. The ATR-FTIR spectrum for the octacalcium phosphate standard (dotted line) is included for comparison.

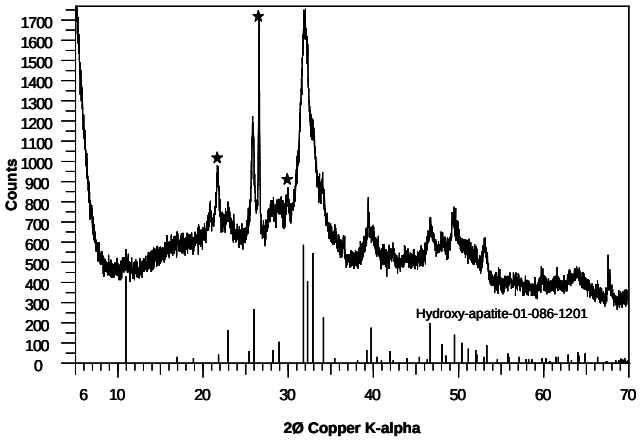

Figure 2. XRPD pattern for Polonite sample from column study (PTE1). The pattern is dominated by peaks due to a hydroxyapatite phase as indicated by comparison to Powder diffraction File reference 'stick' patterns e.g. 01-086-1201. Stars indicate main peaks of minor quartz, cristobalite and wollastonite contamination from the Polonite.

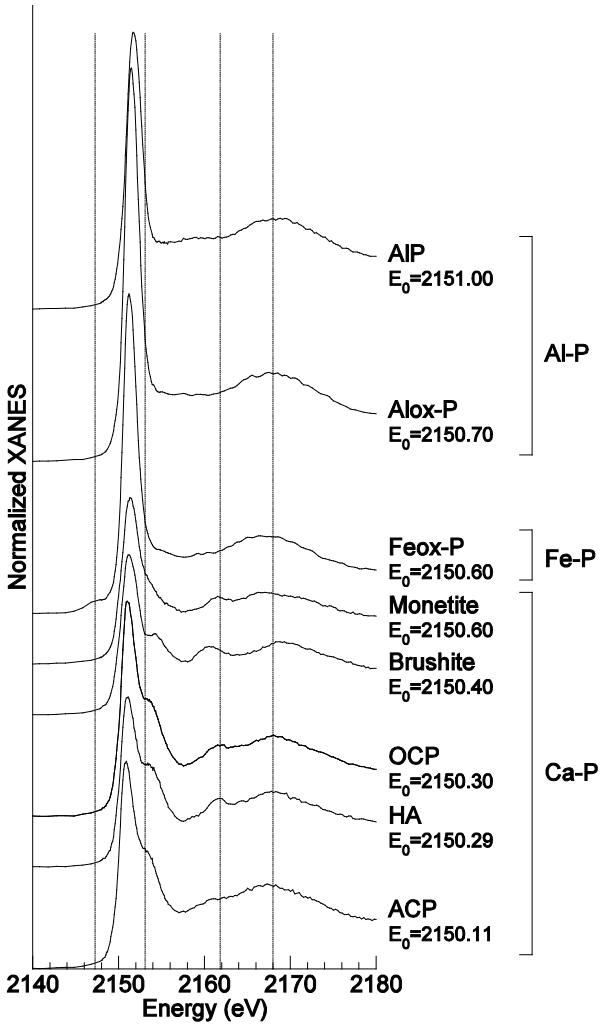

Figure 3. Normalized, stacked P K-XANES spectra for compounds used as standards in linear combination fitting to filter media samples.

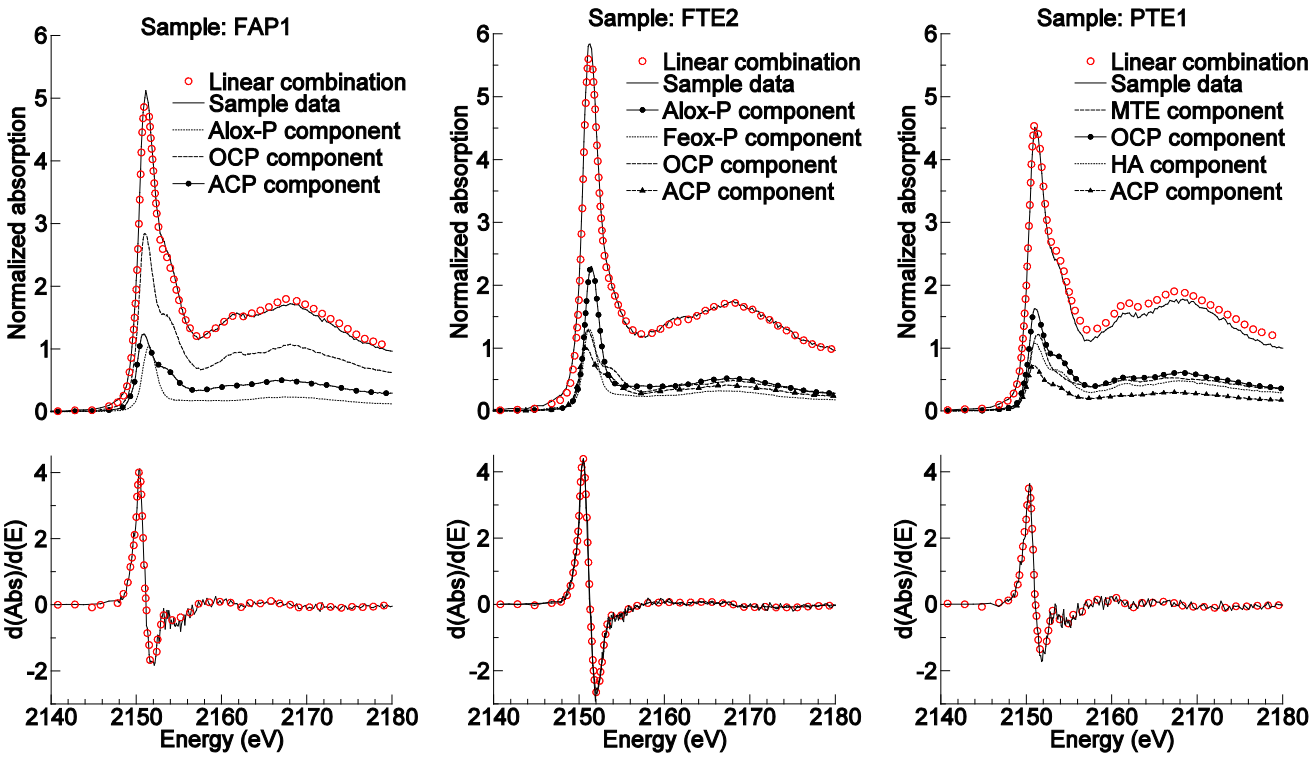

a) b) c)

Figure 4. Linear combinations and sample data in normalized and first derivative space for FAP1 (a), FTE2 (b) and PTE1 (c).

Supporting information

Manuscript title: XANES speciation of P in environmental samples: an assessment of filter media for on-site wastewater treatment.

Authors: David Eveborn*, Jon Petter Gustafsson, Dean Hesterberg, Stephen Hillier

Pages: 5

Number of Figures: 1

Number of Tables: 2

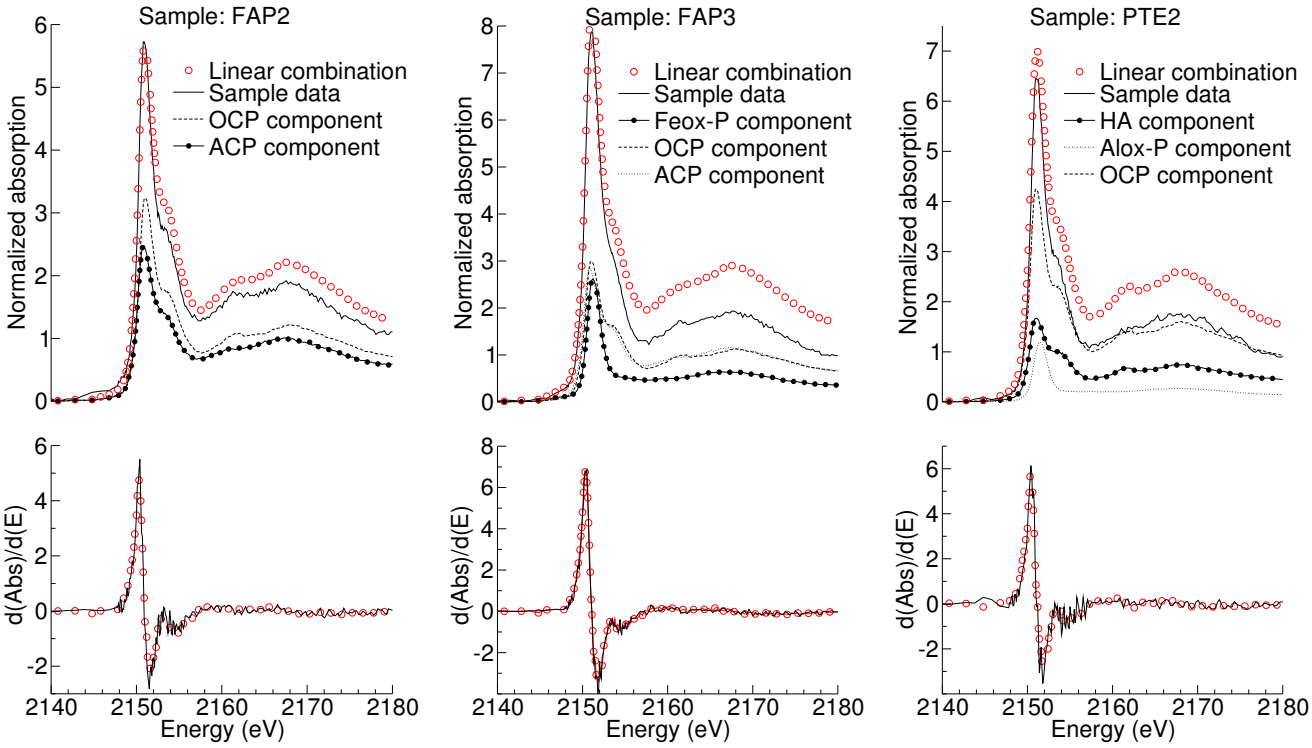
Sample: FAP2
Linear combination
Sample data
OCP component
ACP component
Normalized absorption
d(Abs)/d(E)
Energy (eV)
Sample: FAP3
Linear combination
Sample data
Feox-P component
OCP component
ACP component
Normalized absorption
d(Abs)/d(E)
Energy (eV)
Sample: PTE2
Linear combination
Sample data
HA component
Alox-P component
OCP component
Normalized absorption
d(Abs)/d(E)
Energy (eV)

a) b) c)

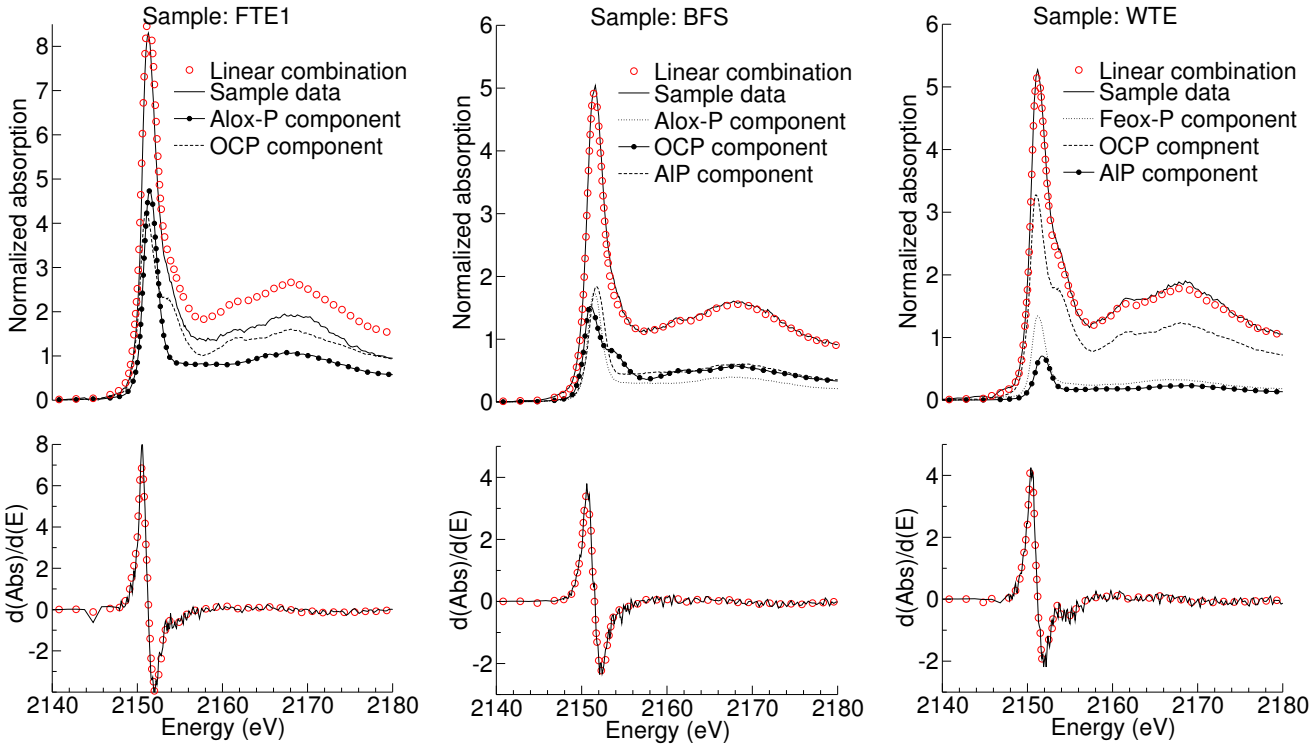
Sample: FTE1
Linear combination
Sample data
Alox-P component
OCP component
Normalized absorption
d(Abs)/d(E)
Energy (eV)
Sample: BFS
Linear combination
Sample data
Alox-P component
OCP component
AlP component
Normalized absorption
d(Abs)/d(E)
Energy (eV)
Sample: WTE
Linear combination
Sample data
Feox-P component
OCP compnent
AlP component
Normalized absorption
d(Abs)/d(E)
Energy (eV)

d) e) f)

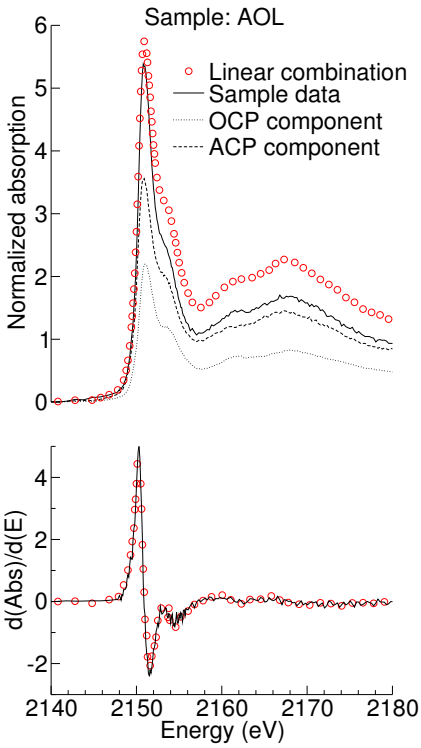

g)

Figure S1. Linear combinations and sample data in normalized and first derivative space for FAP2 (a), FAP3 (b), PTE2 (c), FTE1(d), BFS (e), WTE (f) and AOL (g). Abbreviations: MTE= Monetite, ACP= Amorphous calcium phosphate, OCP= Octacalcium phosphate, HA= Hydroxyapatite, Feox-P=P adsorbed ferrihydrite, Alox-P= P adsorbed to boehmite, AlP=Hydrated aluminium phosphate, FTE=Filtralite, FAP=Filtra P, PTE=Polonite, AOL=Absol, BFS=Blast furnace slag, WTE=Wollastonite

Table S1. Water chemistry parameters of the P-solution (real or synthetic wastewater) used in the loading procedure of the investigated samples as intervals or mean values. Standard deviations in square brackets.

Material	Sample name	BOD_7 (mg dm^{-3})	COD (mg dm-3)	NH_4-N (mg dm^{-3})	Tot-N (mg dm^{-3})	PO_4-P (mg dm^{-3})	pH	Temperature (ºC)
Filtralite P	FTE1	-	-	-	-	10	*	18
	FTE2	130-300	330-630	*	35-90	2-16	*	†
Filtra P	FAP1	-	-	30	30	4.5 [0.9]	6.8 [0.6]	20
	FAP2	*	*	*	*	*	*	†
	FAP3	*	*	*	*	*	*	†
Polonite	PTE1	-	-	30	30	4.5 [0.9]	6.8 [0.6]	20
	PTE2‡	150 [24]	*	35 [14]	69 [11]	5.1 [1.8]	7.8 [0.4]	†
Absol	AOL	*	*	*	*	7.3 [4.0]	7.9 [0.4]	20
Blast furnace slag	BFS	-	-	30	30	4.5 [0.9]	6.8 [0.6]	20
Wollastonite	WTE	-	-	30	30	4.5 [0.9]	6.8 [0.6]	20

* Not known

† Natural variation (mid Sweden)

‡ Data referred from: Renman, A. *On-site wastewater treatment-Polonite and other filter materials for removal of metals, nitrogen and phosphorus*: TRITA-LWR PHD 1043, Doctoral Thesis in Land and Water Resources Engineering; KTH, Architecture and the Built Environment: Stockholm 2008.

Table S2. Component weights for best first-derivative fits in the full range (-5 eV to 30 eV) and in a constrained post-edge region (2 eV to 23 eV). The data are normalized to give a sum of one*.

	ACP		OCP		HA		MTE	
Fitting range (edge-relative eV)	-5 to 30	2-23	-5 to 30	2-23	-5 to 30	2-23	-5 to 30	2-23
FTE1	-	0.56	0.62	0.26	-	-	-	-
FTE2	0.23	0.19	0.29	0.41	-	-	-	-
FAP1	0.27	0.48	0.60	0.43	-	-	-	-
FAP2	0.44	0.36	0.56	0.54	-	0.07	-	-
FAP3	0.38	0.37	0.39	0.25	-	-	-	0.23
PTE1	0.21	0.28	0.47	-	-	0.38	0.32	0.28
PTE2	-	0.60	0.61	0.28	0.30	-	-	-
AOL	0.63	0.59	0.37	-	-	0.26	-	0.12
BFS	-	-	0.39	0.20	-	-	-	0.19
WTE	-	0.18	0.69	0.31	-	-	-	0.27

* Abbreviations: MTE=Monetite, ACP=Amorphous calcium phosphate, OCP=Octa calcium phosphate, HA=Hydroxy apatite, FTE=Filtralite, FAP=Filtra P, PTE=Polonite, AOL=Absol, BFS=Blast furnace slag, WTE=Wollastonite